



Research paper

Synthesis and crystal structures of ZnCl_2 and CdCl_2 containing helical coordination polymers derived from a flexible bis(pyridylurea) ligand

Chao Huang, Xian-Mei Yi, Dong-Mei Chen, Bi-Xue Zhu *

Key Laboratory of Macrocyclic and Supramolecular Chemistry of Guizhou Province, Guizhou University, Guiyang 550025, People's Republic of China

ARTICLE INFO

Article history:

Received 1 September 2017

Received in revised form 22 January 2018

Accepted 26 January 2018

Keywords:

Pyridylurea

Bidentate

Coordination polymer

Helical chain

Racemic

ABSTRACT

A flexible bis(pyridylurea) ligand, 1,1'-[oxybis(2,1-phenylene)] bis(3-pyridin-3-ylurea) (L), has been synthesized and characterized. The interaction of L with ZnCl_2 and CdCl_2 has been investigated. In the structure of $[\{\text{ZnLCl}_2\} \cdot 2\text{DMF}]_n$ (**1**), the flexible ligands bridge the Zn^{II} centers to form 1D helical chains with a pitch of 9.743 Å. The *P* and *M* helical chains are arranged equally, and the whole complex **1** is racemic. In the structure of $[\text{CdLCl}_2(\text{DMF})]_n$ (**2**), the flexible ligands bridge Cd^{II} centers to form one-dimensional *P* and *M* helical chain structures in a similar manner. Then the chlorine atoms act as bridges in bidentate modes linking the *P* helical chain with *M* helical chain to form a 1D looped chain coordination polymer.

© 2018 Elsevier B.V. All rights reserved.

1. Introduction

The synthesis of coordination polymers has attracted much interest in recent years not only because of their intriguing structures, but also for their potential applications in functional solid materials, ion exchange, catalysis, and gas adsorption [1–6], etc. The design strategy for novel self-assembled structures is based on the presence of suitable metal-ligand interactions and supramolecular contacts (hydrogen bonding and $\pi \cdots \pi$ stacking interactions) [7–11]. The flexible ligands could adopt different coordination modes by adjusting their conformation, length, or inherent angle of the terminal coordinative groups, thus leading to fascinating structures of the metal organic frameworks (MOFs) [12–14]. The pyridyl moiety has been proved to be the most popular building block for the construction of metal-organic networks due to its strong coordination ability to metal ions. Among them, the bis(pyridylurea) ligands with both rigid and flexible bridges are ideal units for the construction of various coordination polymers, such as metallomacrocycles, helical chains, and layered networks [15–23].

In this work, the flexible ligand 1,1'-[oxybis(2,1-phenylene)] bis(3-pyridin-3-ylurea) (L) was synthesized by the reaction of 3-isocyanato-pyridine and bis(2-aminophenyl) ether (Scheme 1). Reaction of L with ZnCl_2 or CdCl_2 in DMF/MeOH solution resulted in the formation of 1D helical chain coordination polymer

$[\{\text{ZnLCl}_2\} \cdot 2\text{DMF}]_n$ (**1**) and 1D looped chain coordination polymer $[\text{CdLCl}_2(\text{DMF})]_n$ (**2**).

2. Experimental

2.1. Materials and physical measurements

All commercially available chemicals were of reagent grade and used without further purification. All solvents were purified by conventional methods before use. Elemental analysis was obtained from a Vario EL III elemental analyzer. ^1H NMR spectra was recorded in $\text{DMSO}-d_6$ using a JEOL ECX 400 MHz NMR spectrometer. IR spectra was measured as KBr pellets on a Bio-Rad FTIR instrument at the range of $4000\text{--}400\text{ cm}^{-1}$. The crystal structure was determined by Bruker Smart Apex II CCD and SHELXL crystallographic software of molecular structure.

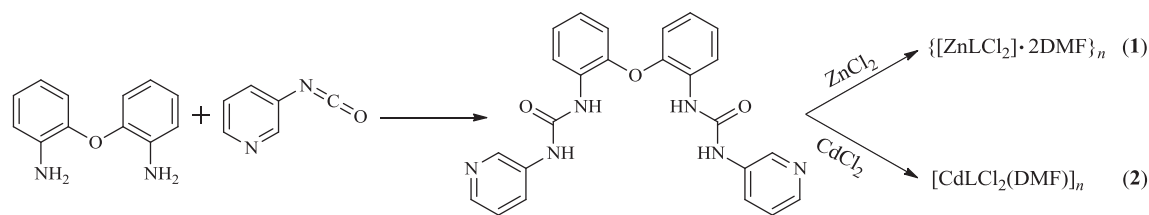
2.2. Synthesis

2.2.1. Synthesis of 1,1'-[oxybis(2,1-phenylene)] bis(3-pyridin-3-ylurea) (L)

L. Nicotinic acid acyl azide and bis(2-aminophenyl) ether were synthesized according to previous literatures [24–26], respectively. A solution of nicotinic acid acyl azide (1.04 g, 7.0 mmol) in toluene (30 mL) was refluxed under nitrogen for 1.5 h, and bis(2-aminophenyl) ether (0.60 g, 3.0 mmol) in acetonitrile (30 mL) was added dropwise. The mixture was stirred for another 1.5 h and cooled to room temperature. The precipitate that formed was collected by filtration and purified by recrystallization from

* Corresponding author.

E-mail address: bxzhu@gzu.edu.cn (B.-X. Zhu).



Scheme 1. Synthesis of the bis(pyridylurea) ligand.

Table 1
Crystal data and structure refinement for the ligand, complexes **1** and **2**.

Compound	L	Complex 1	Complex 2
Empirical formula	C ₂₄ H ₂₀ N ₆ O ₃	C ₃₀ H ₃₄ Cl ₂ N ₈ O ₅ Zn	C ₂₇ H ₂₇ Cl ₂ N ₇ O ₄ Cd
Formula weight	440.46	722.92	696.85
Crystal system	Monoclinic	Monoclinic	Monoclinic
Space group	P2 ₁ /c	P2 ₁ /n	P2 ₁ /c
a/(Å)	10.899(4)	10.832(3)	10.100(16)
b/(Å)	14.206(5)	9.743(3)	9.139(14)
c/(Å)	14.242(5)	32.396(10)	42.820(7)
β/(°)	105.238(8)	93.993(5)	92.038(3)
V/(Å ³)	2127.7(13)	3410.6(17)	3950.1(11)
Z	4	4	4
D _c /(g cm ⁻³)	1.375	1.408	1.172
θ range/(°)	1.94 ~ 25.00	1.26 ~ 26.00	0.95 ~ 27.83
Absorption coefficient/mm ⁻¹	0.095	0.927	0.722
F(0 0 0)	920	1496	1408
Reflections collected	10,650	29,034	36,172
Independent reflections	3732	6683	9305
Observed reflections (I > 2σ(I))	2273	4933	6527
Number of parameters	298	415	372
Goodness-of-fit on F ²	1.078	1.078	1.030
Final R indices (I > 2σ(I))	R ₁ = 0.0590, wR ₂ = 0.1705	R ₁ = 0.0548, wR ₂ = 0.1593	R ₁ = 0.0461, wR ₂ = 0.1230
R indices (all data)	R ₁ = 0.1029, wR ₂ = 0.1898	R ₁ = 0.0763, wR ₂ = 0.1702	R ₁ = 0.0688, wR ₂ = 0.1388
Largest diff. Peak and hole (e Å ⁻³)	0.496 and -0.209	0.894 and -0.489	0.461 and -0.529

CH₃OH/DMF(V: V = 2:1) to give a white solid. Yield: 1.07 g, 81%; mp: 285 ~ 286 °C. ¹H NMR (DMSO-*d*₆, 400 MHz): δ 6.84 (d, 2H, J = 7.6 Hz, Ar-H), 7.02 (t, 2H, J = 5.2 Hz, Ar-H), 7.18 (t, 2H, J = 5.6 Hz, Ar-H), 7.36 (dd, 2H, J = 2.8 Hz, Ar-H), 7.99 (m, 2H, Py-H), 8.23 (d, J = 2.8 Hz, 2H, Py-H), 8.35 (d, J = 6.8 Hz, 2H, Py-H), 8.61 (s, 2H, Py-H), 8.75 (s, 2H, CONH), 9.52 (s, 2H, CONH). ¹³C NMR (DMSO-*d*₆, 400 MHz): δ 152.98, 145.76, 143.53, 140.33, 136.81, 131.60, 125.47, 124.64, 124.15, 123.20, 120.23, 118.38. Anal. Calcd(%) for C₂₄H₂₀N₆O₃: C 65.45, H 4.58, N 19.08; found(%): C 65.49, H 4.62, N 19.03. FT-IR (KBr pellet, ν/cm⁻¹): 3344 (m, NH), 1715 (s, CO), 1599 (s, NH). ESI-MS: *m/z* = 441 [M+H]⁺, 463 [M+Na]⁺.

2.2.2. Synthesis of Zn(II) and Cd(II) complexes

{[ZnLCl₂]·2DMF}_n (1). ZnCl₂ (136 mg, 1 mmol) in methanol (20 mL) was added dropwise with stirring to L (440 mg, 1 mmol) in DMF (20 mL) and stirring was continued at room temperature for 3 h. The initial white precipitate that formed was filtered off. The filtrate was allowed to evaporate slowly at room temperature to yield colorless single crystals that proved suitable for X-ray analysis. The crystalline product was washed and dried under vacuum before analysis. Yield, 42%. Anal. Calcd. (%) for C₃₀H₃₄Cl₂N₈O₅Zn: C 49.84, H 4.74, N 15.50; found (%): C 49.88, H 4.69, N 15.56. FT-IR (KBr pellet, ν/cm⁻¹): 3335 (m, NH), 1711 (s, CO), 1598 (s, NH).

[CdLCl₂(DMF)]_n (2). CdCl₂·2.5H₂O (228 mg, 1 mmol) in methanol (30 mL) was added dropwise with stirring to L (440 mg, 1 mmol) in DMF (20 mL) and stirring was continued at room temperature for 2 h. The solution was filtered off and left for slow evaporation at room temperature. X-ray quality block-shaped colorless crystals were obtained after 5 days. The crystals were collected by filtration, washed with methanol, and dried at room temperature to give complex **2** as a white solid in 38% yield. Anal. Calcd.

(%) for C₂₇H₂₇Cl₂N₇O₄Cd: C 46.54, H 3.91, N 14.07; found(%): C 46.60, H 3.96, N 14.01. FT-IR (KBr pellet, ν/cm⁻¹): 3354 (m, NH), 1714 (s, CO), 1606 (s, NH).

2.3. Crystallographic data collection and structure determination

The single-crystal X-ray diffraction was performed on a Bruker Smart Apex II CCD diffractometer. Intensities of reflections were measured using Mo Kα monochromatized radiation (λ = 0.71 073 Å) at 293(2) K. Data reductions and absorption corrections were performed using the SAINT and SADABS software packages, respectively. The structures were solved by direct methods and refined by full-matrix least-squares methods on F² using the SHELXS-97 and SHELXL-97 [27] programs. Anisotropic thermal factors were assigned to all the non-hydrogen atoms. Crystal data and structure refinement parameters are listed in Table 1. Selected bond lengths and angles for the two complexes are listed in Table 4.

3. Results and discussion

3.1. X-ray structures

3.1.1. Crystal structure of the ligand

Suitable single crystals of free ligand were obtained from MeOH/DMF(1:1 v/v) solution via slow evaporation. The crystal belongs to the centrosymmetric monoclinic space group P2₁/c and its asymmetric unit is comprised of a fully occupied ligand (Fig. 1a). The dihedral angle between the two aromatic rings is 88.05°. The dihedral angles between the central aromatic rings and the neighboring urea moieties are found to be 11.84 and 1.47°, and between urea moieties and the terminal pyridyl rings

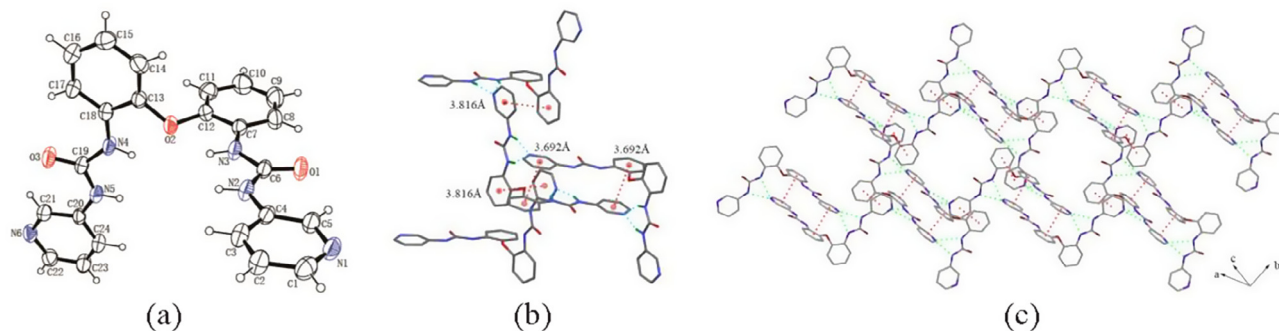


Fig. 1. (a) Molecular structure of the ligand; (b) The hydrogen bonds and π - π stacking interaction in the ligand. Non-urea hydrogen atoms are omitted for clarity; (c) Layered structure in the ab plane formed by $N-H\cdots N$ bonds and π - π stacking interaction.

Table 2

Hydrogen bonding distances (Å) and angles ($^\circ$) for the ligand.

D-H \cdots A	D-H(Å)	H \cdots A(Å)	D \cdots A(Å)	\angle DHA	Symmetry code
N2-H2A \cdots N6 $^{\#1}$	0.8600	2.0787	2.919(3)	165.48	$2-x, -1/2+y, 1/2-z$
N3-H3A \cdots O2	0.8603	2.1930	2.620(3)	110.40	
N3-H3A \cdots N6 $^{\#1}$	0.8603	2.3234	3.124(3)	155.00'	$2-x, -1/2+y, 1/2-z$
N4-H4 \cdots O2	0.8603	2.2664	2.661(3)	107.95	
N4-H4 \cdots N1 $^{\#2}$	0.8603	2.3167	3.125(4)	156.58	$1-x, 1-y, -z$
N5-H5A \cdots N1 $^{\#2}$	0.8596	2.1178	2.959(4)	165.80	$1-x, 1-y, -z$
C5-H5 \cdots O1	0.9298	2.2982	2.914(4)	123.32	
C8-H8 \cdots O1	0.9303	2.3481	2.941(5)	121.34	
C11-H11 \cdots O3 $^{\#3}$	0.9295	2.4125	3.313(4)	163.27	$2-x, 1-y, 1-z$
C17-H17 \cdots O3	0.9297	2.3573	2.932(4)	119.76	
C21-H21 \cdots O3	0.9307	2.2943	2.908(4)	123.03	

are 9.90 and 1.59 $^\circ$. Each ligand molecule is found to be associated with three neighboring ligand molecules via $N-H\cdots N$ hydrogen bonding between the pyridyl N atoms and the urea N atoms. Furthermore, π - π stacking interactions are formed between the pyridyl ring and the aromatic ring with the face-to-face distance of ca. 3.69 and 3.82 Å (Fig. 1b). Through these $N-H\cdots N$ hydrogen bondings and π - π stacking interactions, the structure is linked into a two-dimensional sheet in the ab plane (Fig. 1c) (Table 2).

3.1.2. Crystal structure of complex 1

Slow evaporation of a solution of $ZnCl_2$ and L in MeOH-DMF afforded colorless block crystals of $\{[ZnLCl_2]\cdot 2DMF\}_n$ (**1**). Complex **1** crystallizes in the monoclinic space group $P2_1/n$. The asymmetric unit comprises a independent Zn^{II} center, two chlorine ions, a ligand L, and two solvent DMF molecules (Fig. 2a). In the crystal structure, the zinc centers are each bound to two chlorine ions

and two nitrogen donors from pyridine rings belonging to different ligands. The Zn1-N6 and Zn1-N1a bond lengths are 2.059(3) and 2.078(3) Å. The Zn1-Cl1 and Zn1-Cl2 bond lengths are 2.2092(12) and 2.2215(12) Å. The N-Zn-Cl bond angles are in the range of 104.25(9)-114.63(9), which are distorted from the ideal tetrahedral geometry as a consequence of the opening of the two chloro ligands. The bond angles for Cl1-Zn-Cl2 and N6-Zn-N1a are 123.99(5) and 95.69(12), respectively, which are consistent with those found in similar complexes. The two DMF solvents are bonded to the urea nitrogen atoms via four $N-H\cdots O$ hydrogen bonding ($N\cdots O=2.7603$ - 3.2391 Å) (Fig. 2b). The flexible ligand in complex **1** bridges the Zn^{II} centers to form 1D helical chains running along the b axis with a pitch of 9.743 Å (Fig. 2c). The P and M helical chains are equally arranged, and each helical chain shows the opposite helicity to the neighboring chain so that the whole complex **1** is racemic. In the extended structure of **1**, each helical

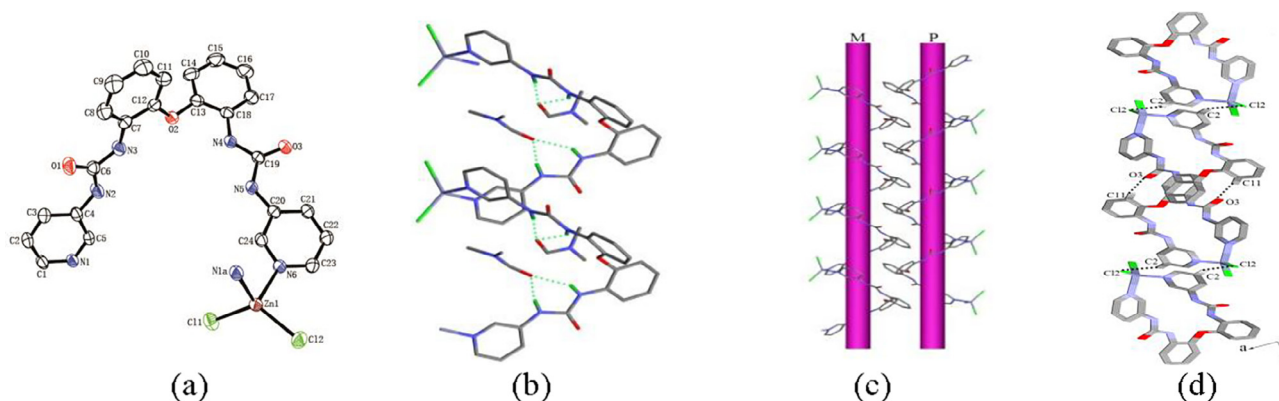


Fig. 2. (a) Coordination environments of the Zn atom in complex **1**. H atoms and lattice DMF molecules are omitted for clarity; (b) $N-H\cdots O$ hydrogen bonds between the urea N atoms and DMF molecules; (c) Racemic helical chains in complex **1**; (d) Racemic helices viewed along the b axis in complex **1**. Symmetry codes: a) $2-x, 1-y, 1-z$.

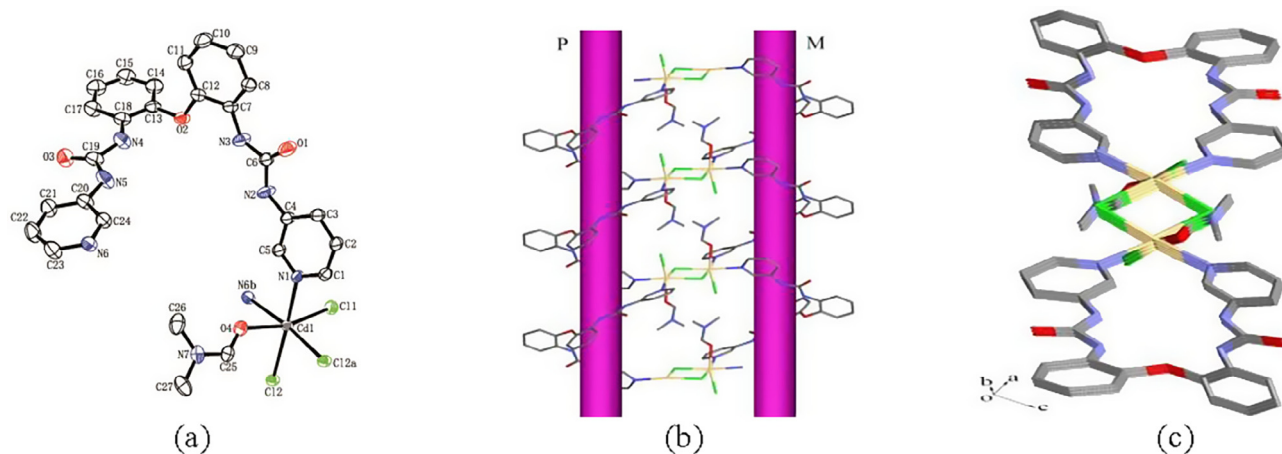


Fig. 3. (a) Coordination environments of the Cd atom in complex **2**. H atoms are omitted for clarity; (b) 1D looped chain structure of complex **2** containing both P and M helical chains; (c) top view along the b axis in complex **2**. Symmetry codes: a) $x, 2 + y, z$; b) $2 - x, 2 - y, 1 - z$.

chain forms C–H···Cl and C–H···O hydrogen bonds with the neighboring chains (Fig. 2d).

3.1.3. Crystal structure of complex **2**

The reaction of L and CdCl₂ in MeOH–DMF (v/v 2:1) gave the complex [CdLCl₂(DMF)]_n (**2**) as colorless block crystals. Complex **2** crystallizes in the monoclinic space group $P2_1/c$. The asymmetric unit of **2** consists of one Cd(II) atom, two chlorine anions, one independent ligand, and one coordinated DMF molecule (Fig. 3a). The cadmium atom is six-coordinated by two nitrogen atoms from two pyridine ring of two different pyridylurea ligands, an oxygen atom from a DMF molecule, two bridged chlorine atom (Cl2, Cl2a) and a terminal chlorine atom (Cl1) in a slightly distorted octahedral geometry. Atoms N(1), N(6b), Cl(2) and Cl(2a) constitute the basal plane of the octahedron, and atoms O(4) and Cl(1) are located at the axial positions [28–30]. All the ligands act as bis(monodentate) bridging ligand linking the Cd(II) ions to form a one-dimensional P and M helical chain structure alternatively. Then the chlorine atoms act as bridges in bidentate modes linking the P helical chain with the M helical chain to form a 1D looped chain coordination polymer (Fig. 3b). The coordination polymer can be considered as a PM type double chain, and each chain shows the same helicity to neighboring double chains. The Cd–Cd distance from one Cd atom to its nearest neighbor through the pyridylurea ligand in the [CdLCl(DMF)]_n chain is 9.139 Å, while the distance between the two Cd atoms bridged by chloride atoms is 3.900 Å (Table 3).

3.2. Powder X-ray diffraction (PXRD)

In order to check the phase purity of the two complexes, the powder X-ray diffraction (PXRD) patterns of complex **1** and **2** were measured at room temperature. As shown in Fig. 4, the peak positions of the simulated and as-synthesized PXRD patterns are in agreement with each other, demonstrating a good phase purity of the two complexes. The difference in reflection intensities between the simulated and experimental patterns was due to the variation in crystal orientation [31,32] or particle size for the powder sample.

3.3. TG analyses of the complexes

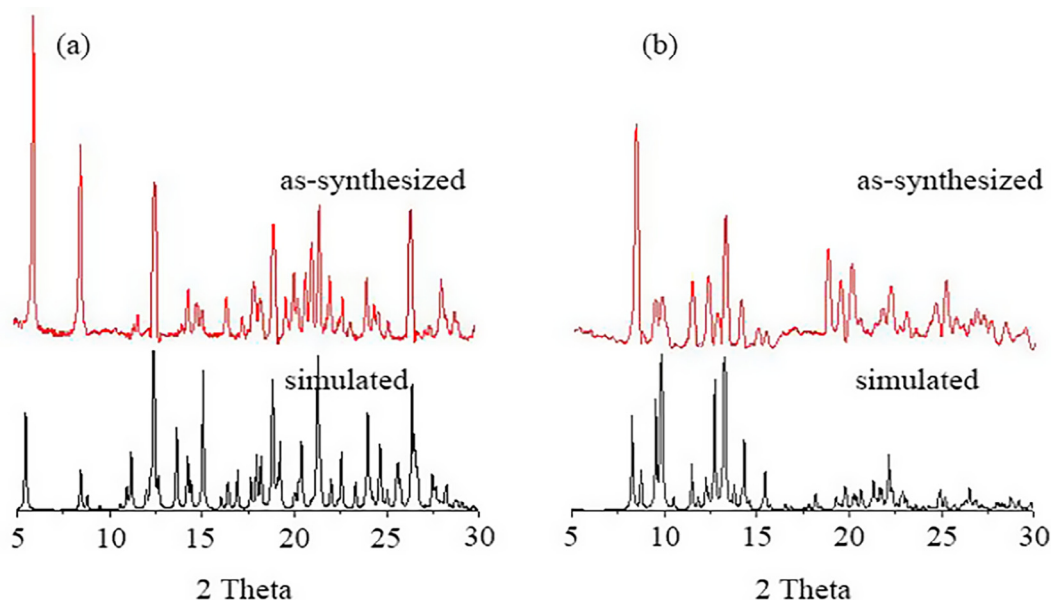
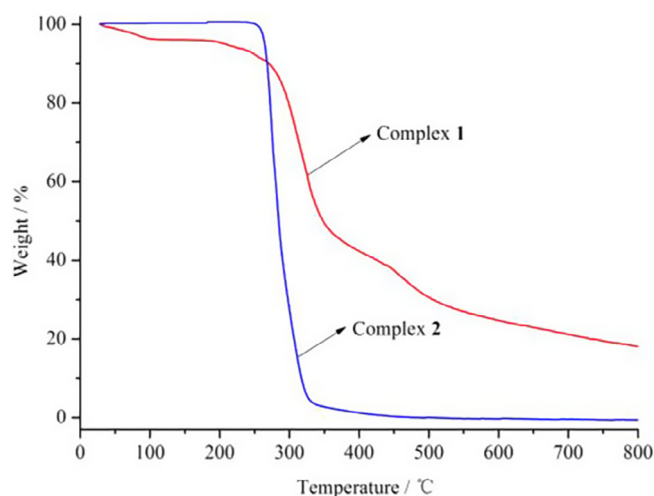
In order to examine the thermal stability of two complexes, TGA experiments for the two complexes were performed between 30 and 800 °C in the N₂ atmosphere at the heating rate of 10 °C·min⁻¹ (Fig. 5). The TG analyses of complex **1** showed a slight weight loss from room temperature to 295 °C corresponding to the release of DMF molecules (observed weight loss 18.1%, calculated 20.1%), as well as a major weight loss occurring at above 300 °C due to the decomposition of the organic ligand. The TGA curve showed complex **2** is stable below 260 °C. Upon further heating, an obvious weight loss (84%) occurs in the temperature range of 260–320 °C, which is corresponding to the loss of coordinated DMF molecules and the decomposition of the organic framework. TGA experiments suggest that complex **2** is more stable than

Table 3
Hydrogen bonding distances (Å) and angles (°) for complex **1**.

D–H···A	D–H(Å)	H···A(Å)	D···A(Å)	∠DHA	Symmetry code
N2–H2···O4 ^{#4}	0.8599	1.9132	2.7603	168.07	–1 + x, y, z
N3–H3···O2	0.8599	2.2635	2.6680	108.81	
N3–H3···O4 ^{#4}	0.8599	2.3228	3.0981	150.10	–1 + x, y, z
N4–H4···O2	0.8599	2.1787	2.6045	110.26	
N4–H4···O5	0.8599	2.4870	3.2391	146.52	
N5–H5···O5	0.8601	1.9817	2.8277	167.60	
C2–H2A···Cl2 ^{#5}	0.9300	2.7457	3.6219	157.40	1/2 – x, –1/2 + y, 1/2 – z
C3–H3A···O1	0.9300	2.3669	2.9217	118.03	
C8–H8···O1	0.9300	2.3382	2.9199	120.29	
C11–H11···O3 ^{#6}	0.9300	2.5407	3.4521	166.57	–x, 2 – y, –z
C17–H17···O3	0.9301	2.3390	2.9213	120.35	
C21–H21···O3	0.9301	2.4102	2.9340	115.56	
C22–H22···O1 ^{#7}	0.9299	2.4169	3.3318	167.88	–1 + x, 1 + y, z
C29–H29B···Cl2 ^{#8}	0.9599	2.7658	3.7128	169.10	1/2 – x, 1/2 + y, 1/2 – z

Table 4
Selected bond distances (Å) and angles (°) for complexes **1** and **2**.

Complex 1					
N6–Zn1	2.059(3)	Cl2–Zn1	2.2215(12)	Zn1–N1a	2.078(3)
Cl1–Zn1	2.2092(12)				
N6–Zn1–N1a	95.69(12)	N6–Zn1–Cl1	114.63(9)	N1a–Zn1–Cl1	104.25(9)
N6–Zn1–Cl2	104.92(9)	N1a–Zn1–Cl2	109.67(9)	Cl1–Zn1–Cl2	123.99(5)
Complex 2					
Cd1–Cl2a	2.6560(10)	Cd1–Cl2	2.6041(9)	Cd1–Cl1	2.5425(11)
Cd1–O4	2.323(3)	Cd1–N6b	2.441(3)	Cd1–N1	2.404(3)
Cl2–Cd1–Cl2a	84.27(3)	Cl1–Cd1–Cl2	102.37(3)	Cl1–Cd1–Cl2a	96.69(3)
O4–Cd1–Cl2	89.80(7)	O4–Cd1–Cl1	93.42(7)	O4–Cd1–Cl1	164.86(7)
O4–Cd1–N6b	79.64(10)	O4–Cd1–N1	82.86(10)	N6b–Cd1–Cl2	92.61(8)
N6b–Cd1–Cl2a	172.42(8)	N6b–Cd1–Cl1	90.71(8)	N1–Cd1–Cl2	171.00(8)
N1–Cd1–Cl2a	90.95(7)	N1–Cd1–Cl1	85.73(8)	N1–Cd1–N6b	91.19(10)

**Fig. 4.** Powder X-ray diffraction patterns: as-synthesized (red) and simulated from the single-crystal diffraction data (black): (a) **1**; (b) **2**.**Fig. 5.** TGA curves of complexes **1** and **2**.

complex **1** below 260 °C, which is mainly due to the structural differences of their helicoidal chains.

4. Conclusion

In summary, A flexible bis(pyridylurea) ligand, 1,1'-[oxybis(2,1-phenylene)] bis(3-pyridin-3-ylurea) (L), has been synthesized and characterized. The interaction of L with Zn(II) ions and Cd(II) ions has been investigated. In the structure of $[[ZnLCl_2] \cdot 2DMF]_n$ (**1**), the flexible ligands bridge the Zn^{II} centers to form 1D helical chains with a pitch of 9.743 Å. The P and M helical chains are arranged equally, and the whole complex **1** is racemic. In the structure of $[CdLCl_2(DMF)]_n$ (**2**), the flexible ligands bridge Cd^{II} centers to form one-dimensional P and M helical chain structures in a similar manner. Then the chlorine atoms act as bridges in bidentate modes linking the P helical chain with M helical chain to form a looped-chain 1D coordination polymer.

Acknowledgments

This research was supported by the “Chun-Hui” Fund of Chinese Ministry of Education (No. Z2016009), and Student’s Platform for Innovation and Entrepreneurship Training Program (No. 201510657050).

Appendix A. Supplementary data

Supplementary data associated with this article can be found, in the online version, at <https://doi.org/10.1016/j.ica.2018.01.028>.

References

- [1] B. Akhuli, T.K. Ghosh, P. Ghosh, *CrystEngComm* 15 (2013) 9472.
- [2] B. Akhuli, P. Ghosh, *Dalton Trans.* 42 (2013) 5818.
- [3] C.D. Jia, W. Zuo, D. Zhang, X.J. Yang, B. Wu, *Chem. Commun.* 52 (2016) 9614.
- [4] M. Paul, N.N. Adarsh, P. Dastidar, *Cryst. Growth Des.* 12 (2012) 4135.
- [5] N.N. Adarsh, P. Dastidar, *Cryst. Growth Des.* 10 (2010) 483.
- [6] S. Banerjee, N.N. Adarsh, P. Dastidar, *Cryst. Growth Des.* 12 (2012) 6061.
- [7] L.G. Ji, Z.W. Yang, Y.X. Zhao, M. Sun, L.P. Cao, X.J. Yang, Y.Y. Wang, B. Wu, *Chem. Commun.* 52 (2016) 7310.
- [8] Q.L. Zhang, Y.L. Huang, H. Xu, B. Tu, B.X. Zhu, *J. Coord. Chem.* 70 (2017) 156.
- [9] S.G. Li, B. Wu, Y.J. Hao, Y.Y. Liu, X.J. Yang, *CrystEngComm* 12 (2010) 2001.
- [10] Z.W. Yang, X.J. Huang, Q.L. Zhao, S.G. Li, B. Wu, *CrystEngComm* 14 (2012) 5446.
- [11] Y.J. Hao, B. Wu, S.G. Li, C.D. Jia, X.J. Huang, X.J. Yang, *CrystEngComm* 13 (2011) 215.
- [12] X.J. Huang, Z.W. Yang, X.J. Yang, Q.L. Zhao, Y.N. Xia, B. Wu, *Inorg. Chem. Commun.* 13 (2010) 1103.
- [13] Y.J. Hao, B. Wu, S.G. Li, B. Liu, C.D. Jia, X.J. Huang, X.J. Yang, *CrystEngComm* 13 (2011) 6285.
- [14] R. Zhang, Y.X. Zhao, J.M. Wang, L.G. Ji, X.J. Yang, B. Wu, *Cryst. Growth Des.* 14 (2014) 544.
- [15] N.N. Adarsh, D.K. Kumar, P. Dastidar, *CrystEngComm* 10 (2008) 1565.
- [16] K. Pandurangan, J.A. Kitchen, S. Blasco, F. Paradisic, T. Gunnlaugsson, *Chem. Commun.* 50 (2014) 10819.
- [17] F.Y. Zhuge, B. Wu, J.J. Liang, J. Yang, Y.Y. Liu, C.D. Jia, C. Janiak, N. Tang, X.J. Yang, *Inorg. Chem.* 48 (2009) 21.
- [18] B. Wu, J.J. Liang, Y.X. Zhao, M.R. Li, S.G. Li, Y.Y. Liu, Y.P. Zhang, X.J. Yang, *CrystEngComm* 12 (2010) 2129.
- [19] R. Zhang, Y.L. Zhang, J.M. Wang, L.G. Ji, X.J. Huang, B. Wu, *Chin. J. Chem.* 31 (2013) 679.
- [20] J.J. Liang, B. Wu, C.D. Jia, X.J. Yang, *CrystEngComm* 11 (2009) 975.
- [21] Z.W. Yang, B. Wu, X.J. Huang, Y.Y. Liu, S.G. Li, Y.N. Xia, C.D. Jia, X.J. Yang, *Chem. Commun.* 47 (2011) 2880.
- [22] Q.L. Zhao, X.J. Yang, C.D. Jia, B. Wu, *Inorg. Chem. Commun.* 13 (2010) 873.
- [23] Q.L. Zhao, X.J. Yang, C.D. Jia, X.J. Huang, B. Wu, *Z. Anorg. Allg. Chem.* 636 (2010) 1998.
- [24] M.C. Naranthatta, D. Das, D. Tripathy, H.S. Sahoo, V. Ramkumar, D.K. Chand, *Cryst. Growth Des.* 12 (2012) 6012.
- [25] J.F.K. Wilshire, *Aust. J. Chem.* 41 (1988) 995.
- [26] U. Hernández-Balderas, N. Andrade-López, J.G. Alvarado-Rodríguez, R. Moreno-Esparza, M. Paneque, *Polyhedron* 90 (2015) 165.
- [27] G.M. Sheldrick, SHELXL-97, Program for Crystal Structure Analysis, University of Göttingen, Germany, 1997.
- [28] M.S. Hain, Y. Fukuda, C.R. Ramírez, B.Y. Winer, S.E. Winslow, R.D. Pike, D.C. Bebout, *Cryst. Growth Des.* 14 (2014) 6497.
- [29] K.Y. Choi, Y.M. Jeon, *Inorg. Chem. Commun.* 6 (2003) 1294.
- [30] K.Z. Guo, G.S. Nan, Z.X. Lian, L.J. Qi, Z.Z. Yu, *Chin. J. Struct. Chem.* 34 (2015) 606.
- [31] Z. Shi, G.H. Li, D. Zhang, J. Hua, S.H. Feng, *Inorg. Chem.* 42 (2003) 2357.
- [32] J.W. Cheng, S.T. Zheng, E. Ma, G.Y. Yang, *Inorg. Chem.* 46 (2007) 10534.